The Unconventional Role of Acid Sphingomyelinase in Regulation of Retinal Microangiopathy in Diabetic Human and Animal Models

Madalina Opreanu,[1,2] Maria Tikhonenko,[1] Svetlana Bozack,[1,2] Todd A. Lydic,[1,2] Gavin E. Reid,[3] Kelly M. McSorley,[1] Andrew Sochacki,[1] Gloria I. Perez,[1] Walter J. Esselman,[2] Timothy Kern,[4] Richard Kolesnick,[5] Maria B. Grant,[6] and Julia V. Busik[1]

OBJECTIVE—Acid sphingomyelinase (ASM) is an important early responder in inflammatory cytokine signaling. The role of ASM in retinal vascular inflammation and vessel loss associated with diabetic retinopathy is not known and represents the goal of this study.

RESEARCH DESIGN AND METHODS—Protein and gene expression profiles were determined by quantitative RT-PCR and Western blot. ASM activity was determined using Amplex Red sphingomyelinase assay. Caveolar lipid composition was analyzed by nano-electrospray ionization tandem mass spectrometry. Streptozotocin-induced diabetes and retinal ischemia-reperfusion models were used in in vivo studies.

RESULTS—We identify endothelial caveolae-associated ASM as an essential component in mediating inflammation and vascular pathology in in vivo and in vitro models of diabetic retinopathy. Human retinal endothelial cells (HREC), in contrast with glial and epithelial cells, express the plasma membrane form of ASM that overlaps with caveolin-1. Treatment of HREC with docosahexaenoic acid (DHA) specifically reduces expression of the caveolae-associated ASM, prevents a tumor necrosis factor-α–induced increase in the ceramide-to-sphingomyelin ratio in the caveolae, and inhibits cytokine-induced inflammatory signaling. ASM is expressed in both vascular and neuroretina; however, only vascular ASM is specifically increased in the retinas of animal models at the vasodegenerative phase of diabetic retinopathy. The absence of ASM in $ASM^{-/-}$ mice or inhibition of ASM activity by DHA prevents acellular capillary formation.

CONCLUSIONS—This is the first study demonstrating activation of ASM in the retinal vasculature of diabetic retinopathy animal models. Inhibition of ASM could be further explored as a potential therapeutic strategy in treating diabetic retinopathy.
Diabetes **60:2370–2378, 2011**

From the [1]Department of Physiology, Michigan State University, East Lansing, Michigan; the [2]Microbiology and Molecular Genetics, Michigan State University, East Lansing, Michigan; the [3]Chemistry and Biochemistry and Molecular Biology, Michigan State University, East Lansing, Michigan; the [4]Department of Medicine, Division of Endocrinology, Case Western Reserve University, Cleveland, Ohio; the [5]Department of Molecular Pharmacology and Chemistry, Sloan-Kettering Institute, New York, New York; and the [6]Department of Pharmacology and Therapeutics, University of Florida, Gainesville, Florida.

Corresponding author: Julia V. Busik, busik@msu.edu.
Received 19 April 2010 and accepted 30 May 2011.

DOI: 10.2337/db10-0550

This article contains Supplementary Data online at http://diabetes.diabetesjournals.org/lookup/suppl/doi:10.2337/db10-0550/-/DC1.

Diabetic retinopathy (DR) is a microvascular and neurodegenerative disorder that induces structural and functional abnormalities in all retinal cells (1). Oxidative stress, activation of protein kinase C, accumulation of polyols, and advanced glycation end products have been long accepted to induce retinal damage (2). In addition, a number of metabolic and molecular abnormalities typical of inflammatory state have been described in the retinas of diabetic animals or patients (3). These include increased vascular permeability and edema; leukocyte accumulation and infiltration; increased inflammatory markers interleukin (IL)-1β and tumor necrosis factor-α (TNF-α) (4); vascular endothelial growth factor (VEGF) (5); intercellular adhesion molecule 1 (ICAM-1) (6); and apoptosis, neovascularization, and attempted vascular repair (7).

Sphingomyelinases are important early responders in inflammatory cytokine signaling that catalyze the hydrolysis of sphingomyelin to the proinflammatory and proapoptotic second messenger ceramide. Acid sphingomyelinase (ASM; EC 3.1.4.12) is a product of a gene designated as sphingomyelin phosphodiesterase 1 located within chromosomal region 11p15.4 (8). It is a soluble glycoprotein of an estimated molecular mass of 72 kDa (9). ASM was initially described as a strictly lysosomal enzyme because of its optimal activity at pH 4.5–5.0. However, recent studies identified an important role for ASM in ceramide-mediated signal transduction (10). This involves the translocation of ASM from intracellular compartments to the outer leaflet of cell membranes. Specifically, ASM activity was localized to caveolar membrane microdomains (11), which are enriched in sphingomyelin and represent an important pool for ceramide production. Hydrolysis of sphingomyelin into ceramide facilitates receptor clustering and enhances inflammatory signal transduction by several receptors that mediate the pathological changes typically associated with DR, such as IL-1β and TNF-α (12,13). Endothelial cells are well recognized to be an important source of ASM (14–16) that secrete copious amounts of ASM in response to inflammatory cytokines (15).

n-3-Polyunsaturated fatty acids (PUFAs), and particularly docosahexaenoic acid (DHA), have the ability to modulate various biological processes involved in retinal vascular inflammation, retinal capillary structure and integrity, and retinal angiogenesis (17). We have previously demonstrated that decrease in DHA is associated with increased inflammatory profile in diabetic retina (18). Total n-3-PUFAs, and especially DHA, were shown to be reduced

in the retina of human diabetic eyes (19), and increasing the retinal levels of n-3-PUFAs reduces pathological retinal angiogenesis (17). DHA suppresses cytokine-induced inflammatory signaling and activation of human retinal endothelial cells (HREC) (20). This pronounced anti-inflammatory effect of DHA was mediated, at least in part, through a reduction in ASM activity and expression (16). The role of ASM pathway as a target of the beneficial action of DHA in preventing retinal endothelial activation, injury, and cell death is not known and represents the goal of this study.

RESEARCH DESIGN AND METHODS

Reagents. Crude trypsin was from Difco (Detroit, MI), lyophilized pancreatic elastase was from Calbiochem (San Diego, CA), streptozotocin (STZ) was from Sigma-Aldrich (St. Louis, MO), and Neutral Protamine Hagedorn (NPH) insulin was from Hospira Inc. (Lake Forest, IL). ASM antibody (Kolesnick laboratory), VEGF antibody (Novus Biologicals, Littleton, CO), caveolin-1 antibody (BD Bioscience, San Jose, CA), lysosomal associated membrane protein 1 (LAMP1) antibody (BD Bioscience), and ICAM-1 antibody (Santa Cruz Biotechnology, Santa Cruz, CA) were used. TNF-α and IL-1β were from R&D Systems (Minneapolis, MN). Methyl-β cyclodextrin (MCD) and commonly used chemicals and reagents were purchased from Sigma-Aldrich. ON-TARGET plus SMART pool sphingomyelin phosphodiesterase 1 and ON-TARGET plus siCONTROL (nontargeting pool) were purchased from Dharmacon (Chicago, IL). RT^2 Profiler PCR Array Mouse Angiogenesis was from SA Biosciences (Frederick, MD). Lipid standards were obtained from Avanti Polar Lipids (Alabaster, AL).

Cell culture. Primary cultures of HREC, human retinal pigment epithelial cells (HRPE), and human Muller cells (HMC) were prepared from the tissue provided by National Disease Research Interchange (Philadelphia, PA), and cultured as described previously (21). DHA (100 μmol/L) was added to cell culture as BSA (5:1 molar ratio) conjugate as described previously (16). BSA and linoleic acid were used as control. Cholesterol depletion and replenishment were performed as described previously (22). Cholesterol levels were measured by the Amplex Red Cholesterol Assay Kit (Molecular Probes, Eugene, OR) (22).

Sphingomyelinase assay. Cells were lysed in the acid lysis buffer (50 mmol/L sodium acetate, pH 5; 1% Triton X-100; 1 mmol/L EDTA) with freshly added protease inhibitor cocktail (Sigma-Aldrich). Sphingomyelinase activity was measured using the Amplex Red sphingomyelinase assay (Molecular Probes) (16).

Western blot. Proteins were extracted as previously described (23), resolved on NuPAGE Novex 10% Bis-Tris gels, transferred to nitrocellulose, and immunoblotted using appropriate antibodies followed by secondary IRDye infrared secondary antibodies (Invitrogen, Molecular Probes). Visualization and quantification were performed by Odyssey infrared imaging system (LI-COR Biosciences, Lincoln, NE).

Immunohistochemistry. Cells were fixed and permeabilized in ice-cold methanol, treated with anti–caveolin-1, ASM, and/or LAMP1 antibodies and corresponding secondary antibodies. ASM and caveolin-1 colocalization was visualized by confocal microscopy and measured with Olympus FluoView 1000 software.

Cells in Fig. 1*D* were fixed in 2% paraformaldehyde in PBS and, where indicated, permeabilized by a 10-min incubation in 0.1% Triton X-100.

Rat retinal samples were fixed in Zinc Fixative (BD Biosciences) for 48 h, washed in PBS, and blocked for 60 min with 3% normal serum in 0.3% Triton X-100 in Tris-buffered saline (TBS). Primary antibody incubation was overnight at 4°C followed by two rinses with TBS + Tween 20 at room temperature.

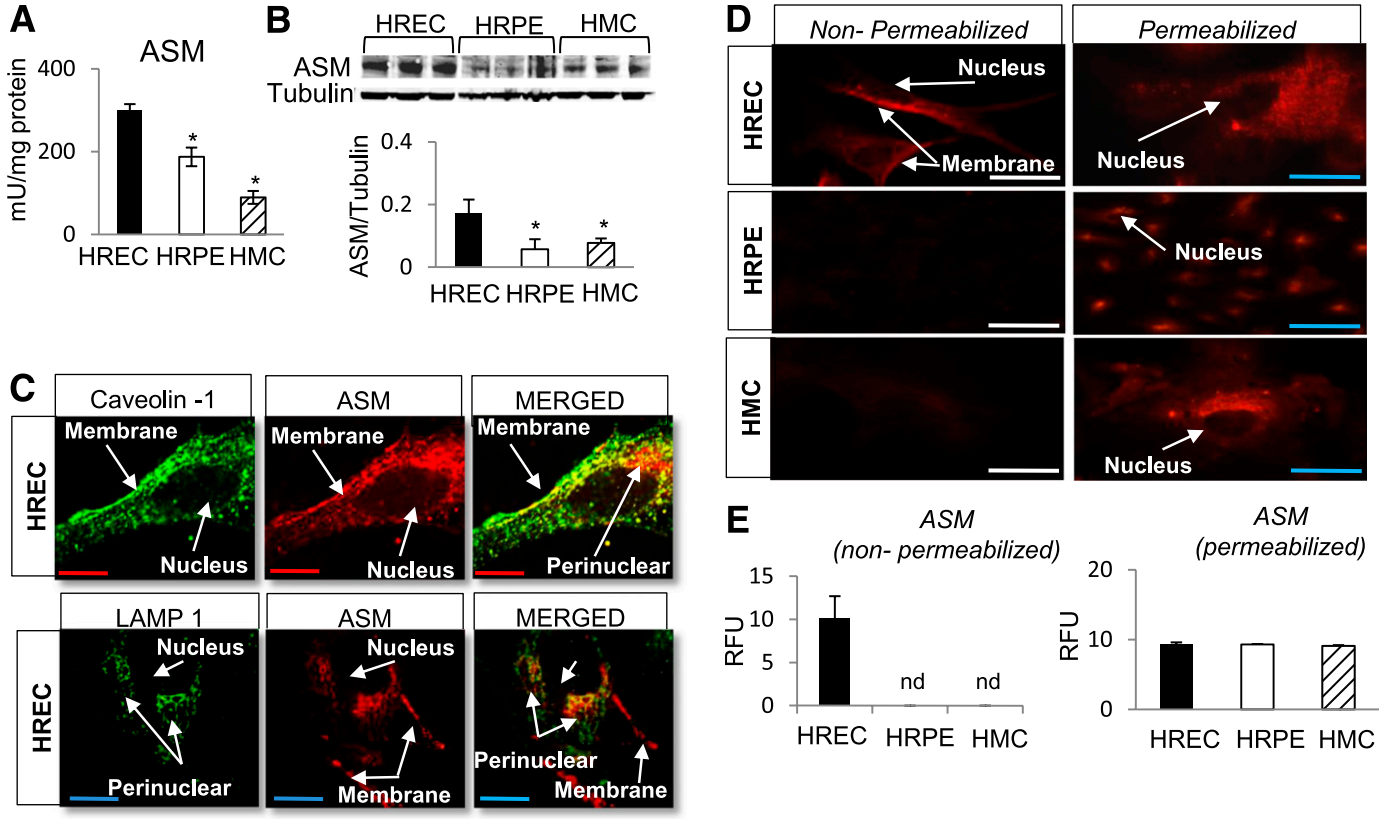

FIG. 1. ASM expression in human retinal cells. ASM activity (*A*) and protein expression (*B*; immunoblot and quantitative analysis) level is the highest in HREC compared with HRPE and HMC. The results are means ± SD of three independent experiments performed in triplicate. *$P < 0.05$ compared with HREC. *C*: ASM, caveolin-1, and LAMP1 colocalization in HREC was assessed by immunohistochemistry. There is 56.38 ± 5.85% colocalization of ASM and caveolin-1 (top) and a strong punctate perinuclear staining, negative for caveolin-1 that associates with LAMP1 (bottom; yellow color in the MERGED panel). *D*: Immunofluorescent staining and quantification of ASM cellular distribution (*E*) in non-permeabilized (left) and permeabilized (right) HREC, HRPE, and HMC. Only HREC express plasma membrane ASM as demonstrated by staining in nonpermeabilized cells (*D*, top left, and quantitation in *E*). ASM staining in permeabilized cells corresponding to ASM in the intracellular compartment is equal in HREC, HRPE, and HMC (*D*, right column, and quantitation in *E*). The results are means ± SD of at least three independent experiments performed in triplicate with eight images in each. RFU, relative fluorescence units. nd, not detected. Red bar = 27.5 μm; blue bar = 55 μm; white bar = 110 μm. (A high-quality digital representation of this figure is available in the online issue.)

Secondary fluorescent antibody incubation was for 3 h at room temperature with rocking, followed by three rinses with TBS + Tween 20.

For colorimetric detection, fixation was followed by automated vacuum infiltrating tissue processing to paraffin block, microtome sectioning, staining on a Dako Autostainer (Dako North America, Carpinteria, CA) for ASM and caveolin-1, and counterstaining with Gill 2 hematoxylin. A Micropublisher 3.3 Megapixel Color Digital Camera was used for imaging, and staining was quantified using a MetaMorph imaging system (Molecular Devices, Downingtown, PA).

Isolation of plasma membrane microdomains. Plasma membrane–enriched fractions and membrane microdomains were prepared using a nondetergent Opti-Prep gradient ultracentrifugation protocol (24) or by a detergent-resistant sucrose gradient ultracentrifugation protocol (22).

Lipid analysis. Whole HREC (3×10^6 cells), HREC membrane microdomain fractions, and plasma membranes were subjected to lipid extraction and nanoelectrospray ionization followed by tandem mass spectrometry of glycerophospholipids and sphingolipids as described previously (25).

Retinal ischemia-reperfusion. All procedures involving the animal models adhered to the ARVO statement for the Use of Animals in Ophthalmic and Vision Research. Retinal ischemia-reperfusion (I/R) was created by temporal increase in intraocular pressure to 90 mmHg as described previously (26). The retinas were isolated either 2 or 7 days after retinal I/R.

Mouse models. Two-month-old male C57BL/6J wild-type ($ASM^{+/+}$) and C57BL/6J ASM-deficient ($ASM^{-/-}$) mice were used.

Rat model. Male Sprague-Dawley rats weighing 300 g were used. The DHA-treated group was on a DHA-enriched diet for 12 days and supplemented via tail vein with 500 nmol/kg DHA 1 day before and 250 nmol/kg DHA (27) immediately before induction of I/R. The control, no treatment group, was on standard rodent diet and subjected to saline solution injection via the tail vein.

Histological assessment of retinal capillaries. Rat and mouse retinal vasculatures were isolated by trypsin (28) or elastase (29) digestion, respectively, and acellular capillaries were systematically counted in the midretina by two independent investigators as described previously (28).

Rat model of type 1 DR. Male Sprague-Dawley rats (237–283 gm) were made diabetic with a single intraperitoneal injection of 65 mg STZ (Sigma-Aldrich) per kg body weight. Starting with day 7 after STZ injection, NPH insulin injections (with a dose of 0–3 units/day) were administered to achieve slow weight gain, but allowing hyperglycemia in the range of 20 mmol/L blood glucose. Body weight and blood glucose concentrations of experimental animals are presented in Table 1.

The experimental diet. AIN-93M purified rodent diet with 10% caloric intake as soybean oil containing 50.8% linoleic acid from Dyets Inc. (Bethlehem, PA) was used as a control diet, and half of the soybean oil, or 5% caloric intake, was replaced with Menhaden oil containing 10.26% DHA and 14.16% eicosapentaenoic acid for the treatment group. A detailed fatty acid composition of the standard rodent diet and DHA-enriched diet is presented in Supplementary Table 1.

Quantitative real-time PCR. Quantitative real-time RT-PCR was performed as described previously (23). Specific primers used for each gene are listed in Supplementary Table 2.

Transferase-mediated dUTP nick-end labeling staining. The TACS-XL Basic In Situ Apoptosis Detection Kit (Trevigen, Gaithersburg, MD) was used on paraffin-embedded sections according to the manufacturer's protocol. After the transferase-mediated dUTP nick-end labeling (TUNEL) assay, the number of TUNEL-positive cells in the ganglion cell layer (GCL) and inner nuclear layer (INL) was quantified on 12 microscopic fields of retinal sections, each 160 μm in length. The number of TUNEL-positive cells was expressed as linear cell density (cells per millimeter) (30).

Statistical analysis. Data are expressed as means ± SE for gene expression measurements and mean ± SD for Western blot quantification, acellular capillary quantification, and ASM vascular expression. Factorial ANOVA with post hoc Tukey test (GraphPad Prism5; GraphPad Software, Inc., San Diego, CA) was used for comparing the data obtained from independent samples. Significance was established at $P < 0.05$.

RESULTS

ASM expression in human retinal cells. To determine which key retinal cell types involved in DR express ASM, we measured the ASM activity and expression levels in HRPE and HMC and compared them with HREC. HREC had the highest ASM activity (Fig. 1*A*) and protein expression levels (Fig. 1*B*) of these cell types. We next examined the distribution of ASM and caveolin-1, the marker of caveolar microdomains, in HREC, HRPE, and HMC. In HREC there was a high degree of colocalization (56.4 ± 5.8%) of ASM and caveolin-1 (Fig. 1*C*, top); however, we also observed a strong punctate perinuclear area that was negative for caveolin-1. This area was confirmed as lysosmal ASM by colocalization with LAMP1 (Fig. 1*C*, bottom). Moreover, although ASM was ubiquitously expressed in the perinuclear lysosomal compartment in HREC, HRPE, and HMC (Fig. 1*D* and *E*), only HREC exhibited pronounced plasma membrane expression of this enzyme (Fig. 1*D* and *E*). Western blot analysis further confirmed colocalization of ASM and caveolin-1 (Fig. 2*C* and Supplementary Fig. 1).

The effect of modification of caveolar lipid composition by DHA on ASM expression in HREC. Previously, we showed that DHA incorporation into the fatty acyl chains of phospholipids in caveolae causes cholesterol displacement from these specialized membrane microdomains (22) and decreases cytokine-induced HREC activation by reducing ASM expression (16).

To prove that DHA-induced modification of caveolar lipid composition specifically controls caveolar sphingomyelinase activity, we determined the effect of cholesterol depletion on ASM activity and expression in HREC. MCD or DHA treatment dramatically decreased cholesterol content of the caveolar fractions in HREC (Fig. 2*A*). MCD treatment had no effect on whole-cell ASM activity, and cholesterol replenishment did not restore whole-cell ASM activity in DHA-treated HREC (Fig. 2*B*). Because a significant portion of cellular ASM is in the lysosomal compartment that would not be affected by MCD and cholesterol treatments used, we next analyzed ASM activity in plasma membrane fraction. ASM activity was significantly decreased in plasma membrane fraction isolated from MCD-treated HREC, and cholesterol replenishment restored ASM activity in the plasma membranes of DHA-treated cells (Fig. 2*B*).

Similar to cholesterol displacement, DHA differentially affected the levels of caveolae versus intracellular ASM. Although DHA treatment of HREC was accompanied by decreased ASM in the caveolar fraction (Fig. 2*C* and Supplementary Fig. 1), there was no effect of DHA on intracellular ASM levels.

TABLE 1
Body weight gain and blood glucose and body weight, blood glucose, and HbA_{1c} of experimental animals with 1 and 9 months of diabetes, respectively

	One month of diabetes		Nine months of diabetes		
	Weight gain (g/day)	Blood glucose (mmol/L)	Weight at the end of the study (g)	Blood glucose (mmol/L)	HbA_{1c} (%)
Control	8.20 ± 1.38	4.8 ± 0.85	733.5 ± 74.24	5.04 ± 0.348	5.3 ± 0.6301
Diabetic control diet	4.13 ± 1.6	25 ± 12.5	547.8 ± 71.87	23.14 ± 4.21	16.228 ± 2.649
Diabetic DHA supplemented diet	4.05 ± 1.79	21.7 ± 13.12	586.83 ± 88.27	18.15 ± 5.023	13.05 ± 3.117

Data are means ± SD.

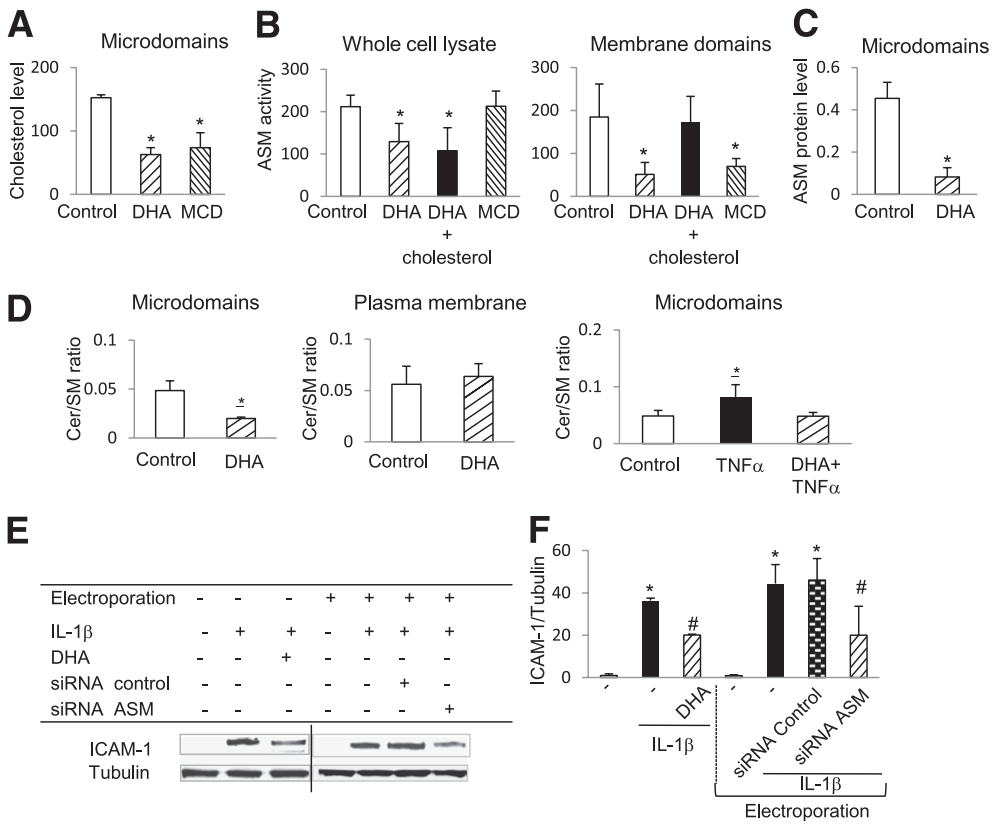

FIG. 2. The effect of DHA and cholesterol depletion on ASM expression in HREC. *A*: DHA and MCD pretreatment of HREC significantly decreased cholesterol content of the caveolar fractions compared with control. *B*: The inhibitory effect of DHA on ASM activity was not mimicked by MCD, and cholesterol replenishment did not restore ASM activity in DHA-treated HREC in whole-cell lysates. However, cholesterol depletion inhibited ASMase activity, and cholesterol replenishment reversed the inhibitory effect of DHA on ASM activity in the plasma membrane fraction. *C*: ASM protein expression in caveolar fractions was isolated from control and DHA-treated HREC. The results are means ± SD of three independent experiments performed in triplicate. *$P < 0.01$ compared with control. *D*: Decrease in ceramide-to-sphingomyelin ratio in caveolae from DHA-treated HREC compared with control. There was no change in ceramide-to-sphingomyelin ratio in total plasma membrane. DHA prevents TNF-α–induced increase in ceramide-to-sphingomyelin ratio in the caveolae. The results are means ± SD of three independent experiments performed in triplicate. *$P < 0.05$ compared with control. *E* and *F*: DHA or ASMase small interfering RNA (siRNA) treatment prevents IL-1β–induced increase in ICAM-1 expression in HREC. Random siRNA was used as control for ASM siRNA experiments. The results are means ± SD of at least three independent experiments performed in triplicate. *$P < 0.05$ compared with control; #$P < 0.05$ compared with IL-1β–stimulated HREC.

Using tandem mass spectrometry analysis of sphingomyelin and ceramide levels, we found a significant decrease in the ceramide-to-sphingomyelin ratio in the caveolar fraction (Fig. 2*D*), but not in the total plasma membrane (Fig. 2*D*), or whole-cell fractions (not shown) isolated from HREC treated with DHA.

Proinflammatory cytokine TNF-α induced an increase in the ceramide-to-sphingomyelin ratio (Fig. 2*D*) in HREC caveolae, and DHA treatment prevented this TNF-α–induced increase and returned the ceramide-to-sphingomyelin ratio to control level.

As we previously reported, ASM small interfering RNA treatment of HREC leads to 94% of ASM gene silencing and reduces total ASM protein level by 50%, whereas pretreatment with 100 μmol/L DHA decreases ASM gene expression by ~50% (16). It is noteworthy that ASM gene silencing recapitulated the effects of DHA on cytokine-induced adhesion molecule expression in HREC, preventing the IL-1β–induced increase in ICAM-1 protein level (Fig. 2*E* and *F*).

Increase in vascular ASM expression after retinal I/R injury in rats. Our cell culture data demonstrate that caveolar ASM expression in endothelial cells, rather than other retinal cells, plays a key role in cytokine-induced endothelial activation. To determine the distribution pattern of ASM in vivo, we performed immunohistochemistry of retinal flat mounts and cross-sections of the retinal layers in rats. Retinal blood vessels exhibited the highest positive staining for ASM (Fig. 3*A* and *B*) in the retina, which colocalized with caveolin-1 (Fig. 3*A*).

Next, we investigated the role of ASM in the activation and degeneration of retinal vessels using a well established model of accelerated I/R injury that closely resembles DR (26). ASM expression was examined in the retinal tissue 2 days after I/R injury. Immunohistochemistry analysis of retinal cross-sections obtained from uninjured and I/R-injured eyes showed that I/R injury specifically increased ASM expression in the retinal vasculature with little or no effect on ASM expression in retinal GCL, INL, and outer nuclear layer (Fig. 3*D* and *E*). Because DHA was an effective ASM inhibitor in our cell culture experiments, we next determined the effect of this n-3-PUFA on ASM expression in the rat retinal tissue isolated from uninjured and I/R-injured eyes. DHA supplementation before retinal injury specifically prevented ASM upregulation in the retinal vasculature (Fig. 3*D* and *E*).

DHA protective effect on I/R-induced retinal neurodegeneration. We next examined the effect of I/R insult on retinal neuronal loss. In accordance with published studies (30,31), we found that retinal I/R resulted in

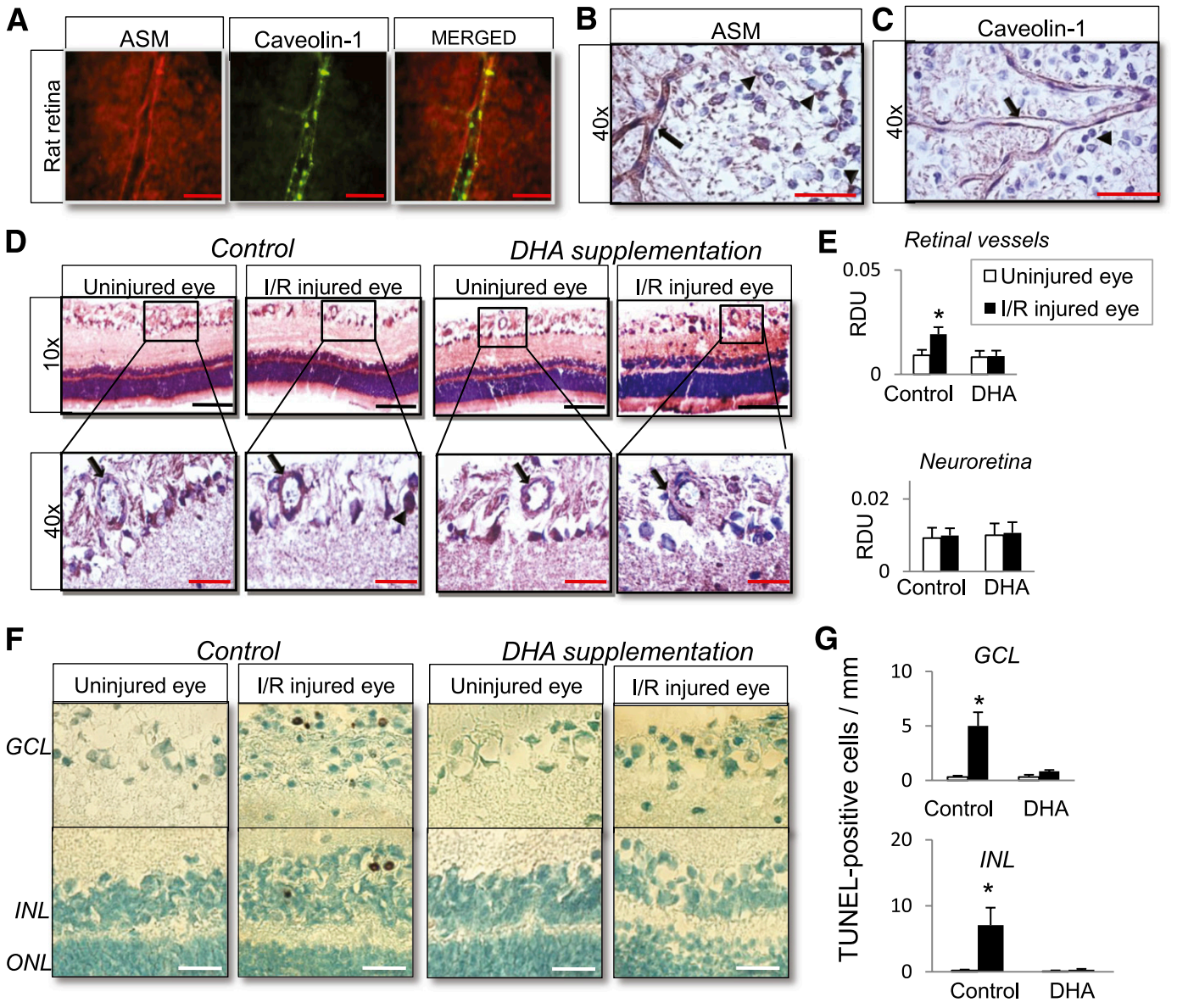

FIG. 3. Increase in vascular ASM expression and apoptosis of neuroretina after retinal I/R injury in rats. *A*: Colocalization of ASM and caveolin-1 in normal rat retina flat mount. *B*: ASM expression in normal rat retina showing ASM-positive staining of retinal vessels (black arrow) and perinuclear lysosomal compartment of retinal ganglion cells (black arrowhead). *C*: Caveolin-1 expression in normal rat retina showing caveolin-1-positive staining of retinal vessels (black arrow). *D*: Specific increase in ASM expression in the rat retinal vessels (black arrow) from I/R-injured eye compared with control. DHA supplementation prevents the increase in vascular ASM expression in I/R-injured eye. *E*: Quantification of ASM staining (normalized to background) in retinal vessels (black arrow) and neuroretina (retinal GCL; black arrowhead). TUNEL staining of retinal sections from control and DHA-supplemented animals after transient retinal ischemia (*F*) is shown. Number of TUNEL-labeled cells in GCL and INL after retinal I/R (*G*) is shown. The data are presented as means ± SE from two independent sets of animals, with five animals, 11–17 retinal vessels per group. *$P < 0.05$ compared with all other groups. RDU, relative densitometry units. ONL, outer nuclear layer. Red bar = 55 μm; black bar = 220 μm; white bar = 40 μm. (A high-quality digital representation of this figure is available in the online issue.)

TUNEL-positive cells in both GCL and INL. It is noteworthy that our study shows that DHA supplementation before retinal I/R significantly prevented the increase in number of TUNEL-positive cells in both retinal layers compared with I/R-injured retinas from control animals (Fig. 3*F* and *G*).

Retinal gene expression and capillary degeneration in mice undergoing retinal I/R injury. To directly address the hypothesis that ASM activation plays a central role in retinal vascular inflammation and vessel loss, we performed I/R injury model using wild-type ($ASM^{+/+}$) and $ASM^{-/-}$ mouse retina. A significant increase in ASM gene expression was observed 2 days after induction of retinal damage in the retinas of wild-type mice undergoing the I/R model (Fig. 4*A*). At this same time point after I/R injury, the expression of ICAM-1, vascular cell adhesion molecule-1 (VCAM-1), IL-1β, TNF-α, and VEGF (Fig. 4*A*) was significantly increased in retinas of wild-type mice. It is noteworthy that this dramatic upregulation of inflammatory markers was entirely prevented in the I/R-injured retinas of $ASM^{-/-}$ mice (Fig. 4*A*). Examination of mouse retinal vasculature in wild-type mice 7 days after I/R injury showed a dramatic increase in the number of acellular capillaries compared with control retinas (Fig. 4*B*). I/R-injured $ASM^{-/-}$ mouse retinas exhibited significantly fewer acellular capillaries compared with the wild type mice (Fig. 4*B*).

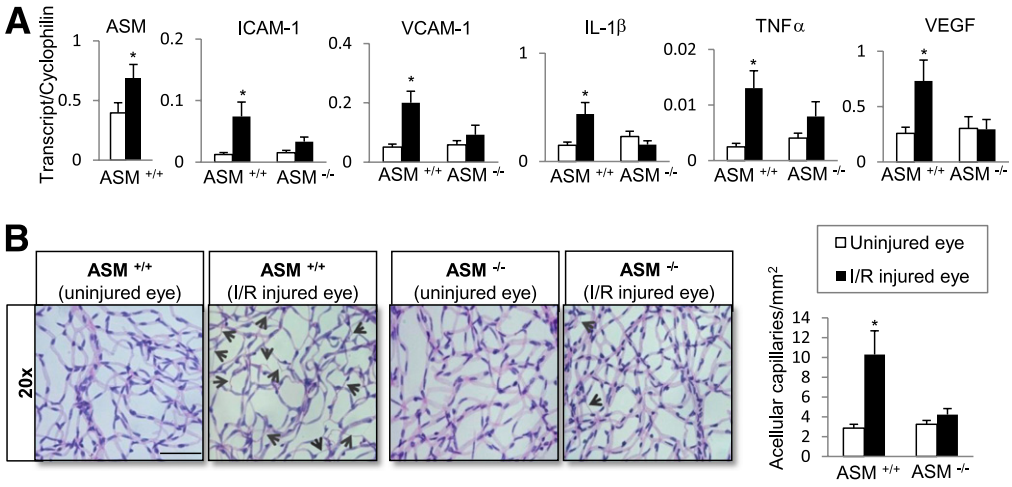

FIG. 4. Retinal gene expression and capillary degeneration in mice undergoing retinal I/R injury. Quantitative PCR analysis of ASM, ICAM-1, VCAM-1, IL-1β, TNF-α, and VEGF (*A*) in retinas isolated from ASM$^{+/+}$ and ASM$^{-/-}$ mice 2 days after retinal I/R injury is shown. The data are presented as means ± SE from three independent sets of mice performed in triplicate with a total of five mice per group. *B*: Acellular capillary occurrence (black arrows) in the retina isolated from ASM$^{+/+}$ and ASM$^{-/-}$ mice 7 days after retinal I/R injury. Quantification of the number of acellular capillaries from five independent sets of mice, with a total of seven mice per ASM$^{+/+}$ group and six mice per ASM$^{-/-}$ group, is shown. At least eight fields of retina were counted in duplicates by two independent investigators. *P < 0.05; black bar = 110 μm. (A high-quality digital representation of this figure is available in the online issue.)

Effect of DHA-supplemented diet on short-term diabetes-induced changes in rat retina. We next used a STZ-induced type 1 diabetic rat model to determine the in vivo effect of diabetes on ASM expression level. ASM gene (Fig. 5*A*) and protein (Fig. 5*B* and *C*) expression dramatically increased in diabetic rat retinas. Moreover, IL-1β, VEGF, and ICAM-1 (Fig. 5*A*) levels were also increased in diabetic retinas. The rats were next subjected to either a control diet or DHA-enriched diet for the duration of the study. In agreement with our cell culture studies and results of the I/R model, DHA reversed ASM induction in the diabetic retina. Significantly, in addition to ASM, DHA-enriched diet prevented the diabetes-induced increase in ICAM-1, VEGF, and IL-1β gene expression (Fig. 5*A*), as well as VEGF protein levels (Fig. 5*B* and *C*).

Effect of DHA-supplemented diet on long-term diabetes-induced degenerative changes in rat retina. To directly determine whether DHA-enriched diet results in protection against development of acellular capillaries, rat retinal vasculature was isolated from 9-month diabetic rats that were subjected to either a DHA-enriched diet or a control diet. Diabetic retinas exhibited a dramatic increase in the numbers of acellular capillaries compared with control retinas (Fig. 6*D*). Retinas from diabetic rats on a DHA-enriched diet showed significantly fewer acellular capillaries compared with retinas from diabetic rats on the control diet (Fig. 6*D*). This protection against vessel loss was associated with a significant reduction in diabetes-induced ASM gene expression (Fig. 6*A*) and ASM protein levels (Fig. 6*B* and *C*), as well as the reduction of

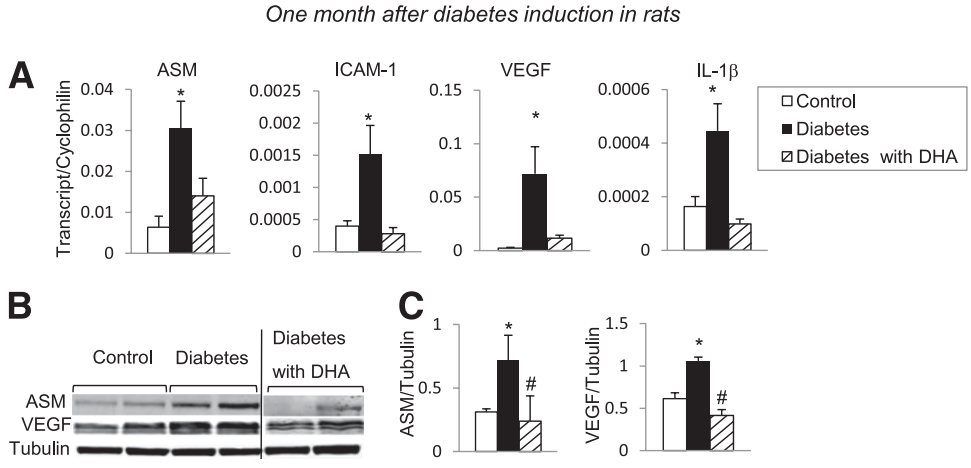

FIG. 5. Effect of DHA-supplemented diet on short-term diabetes-induced changes in rat retina. Retinas isolated 1 month after induction of diabetes were analyzed by quantitative PCR and Western blotting for inflammatory/angiogenic molecule expression levels. Quantitative PCR analysis of ASM, ICAM-1, VEGF, and IL-1β (*A*) from retinas isolated from rats on standard diet (control, white bar; diabetic, black bar) and a DHA-enriched diet (diabetic, striped bar) is shown. The results are means ± SE from three independent sets of animals, with five to eight animals in each group. *P < 0.05 compared with control. Immunoblot (*B*) and quantitative analysis (*C*) of ASM and VEGF protein levels in retinas isolated from control rats on standard diet and from diabetic rats on standard diet or DHA-enriched diet. The results are means ± SD of four animals in each group, performed in triplicate. *P < 0.05 compared with control; #P < 0.05 compared with diabetes.

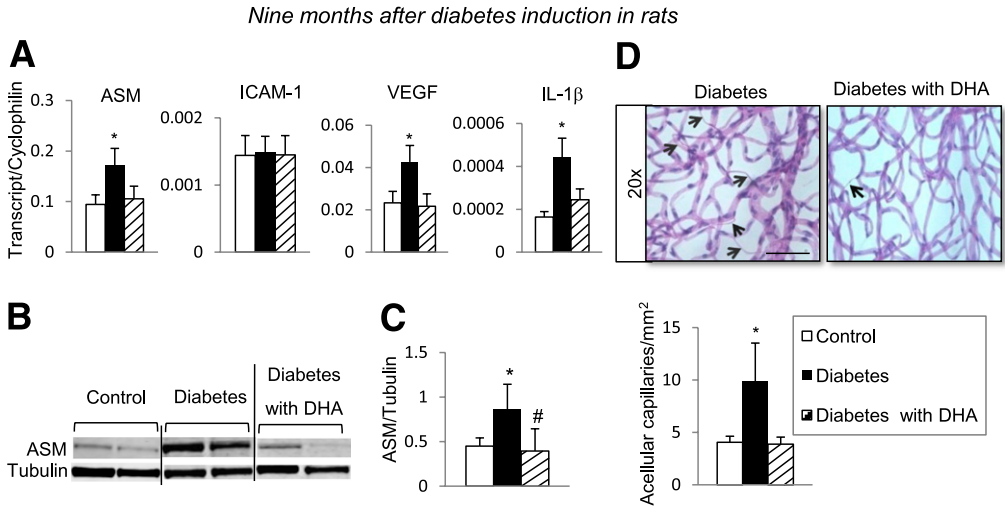

FIG. 6. Effect of DHA-supplemented diet on long-term diabetes-induced degenerative changes in rat retina. Retinas isolated 9 months after induction of diabetes were analyzed by quantitative PCR and immunobloting for inflammatory/angiogenic molecule expression. Quantitative PCR analysis of ASM, ICAM-1, VEGF, and IL-1β (*A*) of retinas isolated from rats subjected to a standard diet (control, white bar; diabetic, black bar) or a DHA-enriched diet (diabetic, striped bar) is shown. The results are means ± SE from one set of animals, with five to eight animals in each group. **P* < 0.05 compared with control. Immunoblot (*B*) and quantitative analysis (*C*) of ASM protein levels in retinas isolated from control rats on standard diet and diabetic rats on standard and DHA-enriched diet. The results are means ± SD of four animals in each group, performed in triplicate. **P* < 0.05 compared with control; #*P* < 0.05 compared with diabetes. *D*: Retinal vasculature from control, diabetic, or diabetic supplemented with DHA animals was prepared using trypsin digestion and stained with hematoxylin and periodic acid–Schiff. Dramatically increased number of acellular capillaries (black arrows) was observed in retinal vasculature isolated from diabetic animals; however, diabetic animals supplemented with DHA were protected from acellular capillaries formation. *D*: Quantification of the total number of acellular capillaries. The results are means ± SD from one set of animals, with eight animals per group. At least eight fields of retina were counted in duplicates by two independent investigators. **P* < 0.05 compared with control; black bar = 110 μm. (A high-quality digital representation of this figure is available in the online issue.)

gene expression for proinflammatory and proangiogenic mediators such as IL-1β and VEGF (Fig. 6*A*). We found no change in ICAM-1 gene expression between the retinas from 9-month diabetic rats and age-matched controls (Fig. 6*A*) as a result of an age-associated increase in ICAM-1 gene expression in control animals.

DISCUSSION

This study has demonstrated for the first time an important role of ASM, the key enzyme in the sphingolipid pathway, in DR.

ASM is classically known to localize to the lysosomal compartment where it has an important role in sphingomyelin lipid storage and degradation. In addition, studies have identified a plasma membrane–associated form of ASM in human fibroblasts (11) and pulmonary vascular endothelial cells (32). Plasma membrane–associated ASM, rather than intracellular ASM, is shown to be associated with inflammatory signaling (33), since ceramide generation within the plasma membrane results in coalescence and reorganization of membrane microdomains into large signaling platforms that facilitate receptor clustering and cellular signal transduction (34,35). In this study, we demonstrate that it is this plasma membrane ASM that is a key element in the retinal inflammatory response in HREC. Our study shows that HREC exhibit high ASM activity and expression level compared with other retinal tissues (Fig. 1*A* and *B*). HREC was the only cell type to demonstrate positive staining for the plasma membrane form of ASM, whereas HRPE and HMC presented only the intracellular form of ASM. Furthermore, immunohistochemistry staining of the retinal blood vessels exhibited the highest positive staining for ASM relative to other retinal layers (Fig. 3*A* and *B*), confirming vascular endothelium as a rich source of ASM.

To corroborate the role of ASM in vascular inflammation and retinal microangiopathy in vivo, we used animal models of retinal I/R and STZ-induced diabetes. First, we used $ASM^{-/-}$ mouse model. As the $ASM^{-/-}$ mouse develops neurodegenerative complications early in life and has a short life span, we are unable to maintain diabetic $ASM^{-/-}$ mouse model for duration of time sufficient to ensure the development of diabetes complications. Therefore, in the $ASM^{-/-}$ mouse, retinopathy was modeled by accelerated retinal I/R injury (26).

Our study shows that retinal I/R injury induces significant upregulation of inflammatory mediators in the retina. Inflammatory mediators can promote the activation and degeneration of capillary endothelial cells with subsequent profound impact on vascular permeability and viability. Indeed, retinas with I/R lesions exhibited a significant number of acellular, degenerated capillaries. Importantly, ASM genetic deficiency decreased proinflammatory/angiogenic mediator gene expression and prevented the development of acellular capillaries in the I/R-injured retinas. We conclude that ASM emerges as a critical initial responder in proinflammatory/angiogenic molecules–induced retinal microvascular degeneration. Analysis of the $ASM^{-/-}$ mouse retinas by RT-PCR showed overall decrease in basal level of angiogenic and inflammatory molecules compared with $ASM^{+/+}$ retinas (Supplementary Fig. 3). Among these, angiopoietin2, endoglin, insulin-like growth factor 1, neuropillin 2, TNF, TNF-α–induced protein 2, connective tissue growth factor, guanine nucleotide–binding protein (α 13), MAD (mothers against decapentaplegic) homolog 5 (Drosophila), TNF ligand superfamily member 12, fibroblast growth factor 1, frizzled homolog 5 (Drosophila), and hypoxia-inducible factor 1 (α subunit) gene expression were found to be more than twofold lower in $ASM^{-/-}$ mouse retinas versus wild-type. We also found more than a twofold

increase in C-fos–induced growth factor (vascular endothelial factor D) and chemokine (C-C motif) ligand 11(eotaxin) gene expression in the retinas from ASM$^{-/-}$ mice; vascular endothelial factor D is mainly involved in formation of lymphatic vessels (36), and eotaxin is considered to be an essential regulator of baseline trafficking of eosinophils (37).

n-3-PUFAs and particularly DHA have been long accepted to modulate inflammatory processes (38). Our recent studies have demonstrated a significant decrease in total n-3-PUFAs, and especially DHA, that was tightly coupled with inflammatory status in the diabetic retina (39). In this study, we found a dramatic increase in retinal gene expression of proinflammatory and proangiogenic mediators, including ASM, IL-1β, and VEGF (Fig. 5*A*). ICAM-1 gene expression was increased threefold in retinas from diabetic rats compared with control (Fig. 5*A*). The upregulation of ASM and other proinflammatory mediators in diabetic retinas was similar to the inflammatory profile of the retinas injured by I/R. Dietary supplementation with DHA prevented diabetic retinal inflammation and vessel loss through, at least in part, inhibition of ASM. Moreover, DHA supplementation before induction of retinal lesions prevented ASM upregulation specifically in the retinal vasculature, with little or no effect on ASM in other retinal tissues (Fig. 3*D* and *E*). It is noteworthy that inhibition of retinal vascular ASM by DHA not only prevented vascular pathology but also decreased the number of TUNEL-positive cells in GCL and INL of the I/R-injured retina. Inhibition of retinal ASM by DHA in diabetic retina recapitulated the effects of ASM deficiency on retinal inflammatory status and the pathology in the I/R-injured mouse eyes.

Available animal models of DR, including chronic STZ-induced diabetes model and accelerated retinal ischemia-reperfusion model used in this study, develop the early degenerative stages of the retinopathy but do not progress to the advanced lesions of the retinopathy. The effect of ASM inhibition and DHA treatment on retinal angiogenesis could not be evaluated in this study and represent the topic of future research (40).

We have previously shown that DHA pretreatment decreases ASM activity and gene expression (16). Our present study demonstrates that DHA incorporation into the fatty acyl chains of phospholipids causes cholesterol displacement from caveolae, thus affecting the ASM protein level in the caveolar microdomain compartment, with no effect on intracellular lysosomal compartment. The decrease of caveolae ASM profoundly affects the ability of HREC to generate ceramide and form ceramide-enriched platforms (41) that augment inflammatory signaling at the plasma membrane receptors level (42). As we previously demonstrated, this treatment does not affect the integrity of caveolae but rather changes caveolar composition to sphingomyelin-rich, low in cholesterol, and ceramide microdomains (22,43). It is noteworthy that G protein-coupled receptor 120 (GPR120) was recently proposed to function as a receptor/sensor for anti-inflammatory effects of DHA (44). Our data would suggest that inhibition of ASM and decreased membrane ceramide and, therefore, membrane remodeling might have a critical impact on the anti-inflammatory effect of DHA via G protein-coupled receptor 120.

Diabetes-induced retinal microvascular damage may be mediated through dyslipidemia and hyperglycemia, two major metabolic abnormalities occurring in diabetes that could activate sphingomyelinases in various tissues (45–49). Numerous studies have demonstrated that at least three major biochemical pathways related to hyperglycemia-induced retinal vascular damage, namely advanced glycation end products production (47), protein kinase C-δ activation (49), and reactive oxygen species generation (45), have the ability to activate sphingomyelinases. As shown by our study, decreased DHA in diabetic retina closely correlates with ASM upregulation and retinal vascular degeneration. ASM and neutral sphingomyelinases (NSM) are both considered major candidates for mediating stress-induced cell injury and death; however, these enzymes have individual requirements for their activation and regulation. ASM functions optimally at a pH of 4.5–5.5, whereas optimal NSM activation occurs at pH of 7.4 and requires magnesium or manganese (10). Diabetic hyperglycemia– and hypoxemia-induced retinal acidosis along with diabetes-related hypomagnesemia (50) may downplay the role of NSM in DR. Our study demonstrates that ASM rather than NSM represents a key player in mediating vascular damage in DR.

Taken together, these in vivo and in vitro data set the stage for developing a more comprehensive understanding of the ASM role in microvascular pathogenesis, where differential regulation of caveolar versus lysosomal ASM expression levels could modulate vascular inflammation and degeneration. We conclude that ASM is a novel and fundamental mediator and a promising therapeutic target for the prevention of retinal vascular inflammation and potentially DR.

ACKNOWLEDGMENTS

This work was supported by grants from the Juvenile Diabetes Research Foundation (2-2005-97 to J.V.B.), National Institutes of Health (EY-016077 to J.V.B., RR-025386 to G.E.R. and J.V.B., EY-012601 and EY-007739 to M.B.G., and DK-090730 to M.B.G. and J.V.B.), MEAS (MICL02163 to J.V.B.), and Michigan State University (OVPRGS to J.V.B.).

No potential conflicts of interest relevant to this article were reported.

M.O. researched data, contributed to the discussion, wrote the manuscript, and reviewed and edited the manuscript. M.T. and T.K. researched data and contributed to the discussion. S.B. and T.A.L. researched data, contributed to the discussion, and reviewed and edited the manuscript. G.E.R. researched data and contributed to the discussion. K.M.M. and A.S. researched data. G.I.P. researched data and wrote the manuscript. W.J.E. wrote the manuscript and reviewed and edited the manuscript. R.K. reviewed and edited the manuscript. M.B.G. contributed to the discussion, wrote the manuscript, and reviewed and edited the manuscript. J.V.B. researched data, contributed to the discussion, wrote the manuscript, and reviewed and edited the manuscript.

Parts of this study were presented in abstract form at the Keystone Conference 2009, Vancouver, British Columbia, Canada, 24 February–1 March 2009, and ARVO Conference 2009, Fort Lauderdale, Florida, 3–7 May 2009.

The authors thank Dr. Arthur Weber (Michigan State University) for his assistance with light microscopy and Sergio Caballero (University of Florida) for assistance with the I/R model. The authors acknowledge the technical support provided by Amy S. Porter, Kathleen A. Joseph, and Ricky A. Rosebury (the Michigan State University Investigative HistoPathology Laboratory-Research Facility) for histology preparations of retinal vasculature.

REFERENCES

1. Imai H, Singh RS, Fort PE, Gardner TW. Neuroprotection for diabetic retinopathy. Dev Ophthalmol 2009;44:56–68
2. Adamis AP, Berman AJ. Immunological mechanisms in the pathogenesis of diabetic retinopathy. Semin Immunopathol 2008;30:65–84
3. Kern TS. Contributions of inflammatory processes to the development of the early stages of diabetic retinopathy. Exp Diabetes Res 2007;2007: 95103.
4. Joussen AM, Poulaki V, Mitsiades N, et al. Nonsteroidal anti-inflammatory drugs prevent early diabetic retinopathy via TNF-alpha suppression. FASEB J 2002;16:438–440
5. Yang LP, Sun HL, Wu LM, et al. Baicalein reduces inflammatory process in a rodent model of diabetic retinopathy. Invest Ophthalmol Vis Sci 2009;50: 2319–2327
6. Nozaki M, Ogura Y, Hirabayashi Y, Saishin Y, Shimada S. Enhanced expression of adhesion molecules of the retinal vascular endothelium in spontaneous diabetic rats. Ophthalmic Res 2002;34:158–164
7. Miyamoto K, Khosrof S, Bursell SE, et al. Prevention of leukostasis and vascular leakage in streptozotocin-induced diabetic retinopathy via intercellular adhesion molecule-1 inhibition. Proc Natl Acad Sci USA 1999; 96:10836–10841
8. Simonaro CM, Park JH, Eliyahu E, Shtraizent N, McGovern MM, Schuchman EH. Imprinting at the SMPD1 locus: implications for acid sphingomyelinase-deficient Niemann-Pick disease. Am J Hum Genet 2006;78:865–870
9. The Diabetic Retinopathy Vitrectomy Study Research Group. Early vitrectomy for severe proliferative diabetic retinopathy in eyes with useful vision. Clinical application of results of a randomized trial—Diabetic Retinopathy Vitrectomy Study Report 4. Ophthalmology 1988;95:1321–1334
10. Marchesini N, Hannun YA. Acid and neutral sphingomyelinases: roles and mechanisms of regulation. Biochem Cell Biol 2004;82:27–44
11. Liu P, Anderson RG. Compartmentalized production of ceramide at the cell surface. J Biol Chem 1995;270:27179–27185
12. Ko YG, Lee JS, Kang YS, Ahn JH, Seo JS. TNF-alpha-mediated apoptosis is initiated in caveolae-like domains. J Immunol 1999;162:7217–7223
13. Martin MU, Wesche H. Summary and comparison of the signaling mechanisms of the Toll/interleukin-1 receptor family. Biochim Biophys Acta 2002;1592:265–280
14. Andrieu-Abadie N, Levade T. Sphingomyelin hydrolysis during apoptosis. Biochim Biophys Acta 2002;1585:126–134
15. Marathe S, Schissel SL, Yellin MJ, et al. Human vascular endothelial cells are a rich and regulatable source of secretory sphingomyelinase. Implications for early atherogenesis and ceramide-mediated cell signaling. J Biol Chem 1998;273:4081–4088
16. Opreanu M, Lydic TA, Reid GE, McSorley KM, Esselman WJ, Busik JV. Inhibition of cytokine signaling in human retinal endothelial cells through downregulation of sphingomyelinases by docosahexaenoic acid. Invest Ophthalmol Vis Sci 2010;51:3253–3263
17. Connor KM, SanGiovanni JP, Lofqvist C, et al. Increased dietary intake of omega-3-polyunsaturated fatty acids reduces pathological retinal angiogenesis. Nat Med 2007;13:868–873
18. Tikhonenko M, Lydic TA, Wang Y, et al. Remodeling of retinal fatty acids in an animal model of diabetes: a decrease in long-chain polyunsaturated fatty acids is associated with a decrease in fatty acid elongases Elovl2 and Elovl4. Diabetes 2010;59:219–227
19. Futterman S, Kupfer C. The fatty acid composition of the retinal vasculature of normal and diabetic human eyes. Invest Ophthalmol 1968;7:105–108
20. Chen W, Esselman WJ, Jump DB, Busik JV. Anti-inflammatory effect of docosahexaenoic acid on cytokine-induced adhesion molecule expression in human retinal vascular endothelial cells. Invest Ophthalmol Vis Sci 2005; 46:4342–4347
21. Busik JV, Mohr S, Grant MB. Hyperglycemia-induced reactive oxygen species toxicity to endothelial cells is dependent on paracrine mediators. Diabetes 2008;57:1952–1965
22. Chen W, Jump DB, Esselman WJ, Busik JV. Inhibition of cytokine signaling in human retinal endothelial cells through modification of caveolae/lipid rafts by docosahexaenoic acid. Invest Ophthalmol Vis Sci 2007;48:18–26
23. Agardh E, Gustavsson C, Hagert P, Nilsson M, Agardh CD. Modifying a standard method allows simultaneous extraction of RNA and protein, enabling detection of enzymes in the rat retina with low expressions and protein levels. Metabolism 2006;55:168–174
24. Macdonald JL, Pike LJ. A simplified method for the preparation of detergent-free lipid rafts. J Lipid Res 2005;46:1061–1067
25. Busik JV, Reid GE, Lydic TA. Global analysis of retina lipids by complementary precursor ion and neutral loss mode tandem mass spectrometry. Methods Mol Biol 2009;579:33-70.
26. Zheng L, Gong B, Hatala DA, Kern TS. Retinal ischemia and reperfusion causes capillary degeneration: similarities to diabetes. Invest Ophthalmol Vis Sci 2007;48:361–367
27. Huang WL, King VR, Curran OE, et al. A combination of intravenous and dietary docosahexaenoic acid significantly improves outcome after spinal cord injury. Brain 2007;130:3004–3019
28. Kern TS, Tang J, Mizutani M, et al. Response of capillary cell death to aminoguanidine predicts the development of retinopathy: comparison of diabetes and galactosemia. Invest Ophthalmol Vis Sci 2000;41:3972–3978
29. Laver NM, Robison WG Jr, Pfeffer BA. Novel procedures for isolating intact retinal vascular beds from diabetic humans and animal models. Invest Ophthalmol Vis Sci 1993;34:2097–2104
30. Kaneda K, Kashii S, Kurosawa T, et al. Apoptotic DNA fragmentation and upregulation of Bax induced by transient ischemia of the rat retina. Brain Res 1999;815:11–20
31. Nishijima K, Ng YS, Zhong L, et al. Vascular endothelial growth factor-A is a survival factor for retinal neurons and a critical neuroprotectant during the adaptive response to ischemic injury. Am J Pathol 2007;171:53–67
32. Yang Y, Yin J, Baumgartner W, et al. Platelet-activating factor reduces endothelial nitric oxide production: role of acid sphingomyelinase. Eur Respir J 2010;36:417-427
33. Schuchman EH. Acid sphingomyelinase, cell membranes and human disease: Lessons from Niemann-Pick disease. FEBS Lett 2010;584:1895-1900
34. Grassmé H, Jendrossek V, Riehle A, et al. Host defense against Pseudomonas aeruginosa requires ceramide-rich membrane rafts. Nat Med 2003;9: 322–330
35. Gulbins E, Grassmé H. Ceramide and cell death receptor clustering. Biochim Biophys Acta 2002;1585:139–145
36. Stacker SA, Caesar C, Baldwin ME, et al. VEGF-D promotes the metastatic spread of tumor cells via the lymphatics. Nat Med 2001;7:186–191
37. Matthews AN, Friend DS, Zimmermann N, et al. Eotaxin is required for the baseline level of tissue eosinophils. Proc Natl Acad Sci USA 1998;95:6273–6278
38. Calder PC. n-3 Polyunsaturated fatty acids, inflammation, and inflammatory diseases. Am J Clin Nutr 2006;83(Suppl.):1505S–1519S
39. Tikhonenko M, Lydic TA, Wang Y, et al. Remodeling of retinal fatty acids in an animal model of diabetes: a decrease in long chain polyunsaturated fatty acids is associated with a decrease in fatty acid elongases Elovl2 and Elovl4. Diabetes 2010;59:219-227
40. Kern TS. In vivo models of diabetic retinopathy. In *Diabetic Retinopathy*. Duh E, Ed. Totowa, NJ, Humana Press, 2008, p. 137–159
41. Kolesnick RN, Goñi FM, Alonso A. Compartmentalization of ceramide signaling: physical foundations and biological effects. J Cell Physiol 2000; 184:285–300
42. Grassmé H, Riethmüller J, Gulbins E. Biological aspects of ceramide-enriched membrane domains. Prog Lipid Res 2007;46:161–170
43. Opreanu M, Lydic TA, Reid GE, McSorley KM, Esselman WJ, Busik J. Docosahexaenoic acid inhibits cytokine signaling in human retinal endothelial cells by downregulating sphingomyelinases. Invest Ophthalmol Vis Sci 2010;51:3253-3263
44. Oh DY, Talukdar S, Bae EJ, et al. GPR120 is an omega-3 fatty acid receptor mediating potent anti-inflammatory and insulin-sensitizing effects. Cell 2010;142:687–698
45. Dumitru CA, Zhang Y, Li X, Gulbins E. Ceramide: a novel player in reactive oxygen species-induced signaling? Antioxid Redox Signal 2007;9:1535–1540
46. Górska M, Barańczuk E, Dobrzyń A. Secretory Zn2+-dependent sphingomyelinase activity in the serum of patients with type 2 diabetes is elevated. Horm Metab Res 2003;35:506–507
47. Patschan S, Chen J, Polotskaia A, et al. Lipid mediators of autophagy in stress-induced premature senescence of endothelial cells. Am J Physiol Heart Circ Physiol 2008;294:H1119–H1129
48. Samad F, Hester KD, Yang G, Hannun YA, Bielawski J. Altered adipose and plasma sphingolipid metabolism in obesity: a potential mechanism for cardiovascular and metabolic risk. Diabetes 2006;55:2579–2587
49. Zeidan YH, Wu BX, Jenkins RW, Obeid LM, Hannun YA. A novel role for protein kinase Cdelta-mediated phosphorylation of acid sphingomyelinase in UV light-induced mitochondrial injury. FASEB J 2008;22:183–193
50. Pham PC, Pham PM, Pham SV, Miller JM, Pham PT. Hypomagnesemia in patients with type 2 diabetes. Clin J Am Soc Nephrol 2007;2:366–373